Journal of the Korean Magnetic Resonance Society **2016**, *20*, 109-113
DOI 10.6564/JKMRS.2016.20.4.109

^{113}Cd and ^{133}Cs NMR Study of Nucleus-Phonon Interactions in Linear-Chain Perovskite-Type $CsCdBr_3$

Sung Soo Park[1,2] and Ae Ran Lim[1,2,*]

[1]Analytical Laboratory of Advanced Ferroelectric Crystals, Jeonju University, Jeonju 55069, Korea
[2]Department of Science Education, Jeonju University, Jeonju 55069, Korea

Received Oct 12, 2016; Revised Nov 23, 2016; Accepted Dec 2, 2016

Abstract Resonance frequencies from the ^{113}Cd and ^{133}Cs nuclear magnetic resonance (NMR) spectra for the $CsCdBr_3$ single crystal were measured at varying temperatures by the static NMR method. The temperature-dependent changes of these frequencies are related to the changing structural geometry of the $CdBr_6^{4-}$ units, which affects the environment of ^{133}Cs. The spin-lattice relaxation rates ($1/T_1$) for the ^{113}Cd and ^{133}Cs nuclei were measured in order to obtain detailed information about the dynamics of $CsCdBr_3$ crystals. The dominant relaxation mechanisms for ^{113}Cd and ^{133}Cs nuclei are direct single-phonon and Raman spin-phonon processes, respectively.

Keywords $CsCdBr_3$, Perovskite, Nuclear magnetic resonance, Nucleus-phonon interaction

Introduction

Many crystallographic studies have been carried out on crystals of perovskite-type compounds with the general formula AMX_3, where X is a halide and A and M are monovalent and divalent metal ions, respectively.[1-4] The perovskite AMX_3 crystals doped with transition metal ions have recently received much attention, because of their particular structures, phase transitions, and luminescence properties.[5] In the case of $CsCdBr_3$, the crystal structure belongs to the space group D_{6h}^4 with two formulae units per unit cell. The crystal is composed of chains of $CdBr_6^{4-}$ octahedra sharing opposite faces, and the chains are aligned along the crystallographic c-axis. Since the separation between the neighboring Cd^{2+} ions is much smaller than that between adjacent $CdBr_6^{4-}$ chains, the crystal has a quasi-one-dimensional structure along the c-axis. Because of a trigonal distortion of the $CdBr_6^{4-}$ unit, the distance between the Br^- ions aligned in the direction perpendicular to the c-axis is smaller than that aligned along the c-axis. The linear chains of slightly deformed $CdBr_6^{4-}$ octahedra are connected through the Cs^+ ions.[6] With such an interesting structure, $CsCdBr_3$ doped with rare-earth ions[7-15] is intensively studied as a promising high-efficiency converter of semiconductor laser radiation.[16,17] At room temperature, $CsCdBr_3$ has the space group $P6_3/mmc$. In the ideal crystal, the $CdBr_6^{4-}$ octahedra would be connected into infinitely long chains, as shown in figure 1. The lattice parameters are a=b=7.675 Å,

* Correspondence to : **Ae Ran Lim**, Department of Science Education, Jeonju University, 303 Cheonjam-ro, Wansan-gu, Jeonju-si, 55069, Korea, Tel: +82-63-220-2514, E-mail: aeranlim@hanmail.net, arlim@jj.ac.kr

c=6.722 Å, α=β= 0°, and γ=120°.[18]

In this study, we obtained the temperature dependences of the resonance frequencies in ^{113}Cd and ^{133}Cs nuclear magnetic resonance (NMR) spectra of $CsCdBr_3$ single crystal by the static NMR method. In order to obtain detailed information about the dynamics of $CsCdBr_3$ crystals, we measured the spin-lattice relaxation rates, $1/T_1$, in the laboratory frame for the constituent ^{113}Cd and ^{133}Cs nuclei. These observed NMR characteristics of $CsCdBr_3$ crystals were used to investigate the vibrational processes within the crystal.

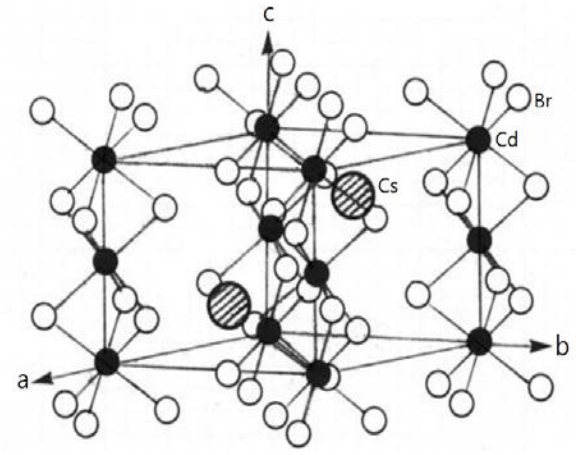

Figure 1. The crystal structure of $CsCdBr_3$ at room temperature.

Experimental Procedure

Single crystals of $CsCdBr_3$ were grown at room temperature by slow evaporation of an aqueous solution containing CsBr and $CdBr_2$•$4H_2O$. The $CsCdBr_3$ crystals were hexagonal, transparent, and colorless.

The static ^{113}Cd and ^{133}Cs NMR spectra for $CsCdBr_3$ crystals were obtained using the Bruker DSX 400 FT NMR spectrometer at the Western Seoul Center, Korea Basic Science Institute. The static magnetic field was 9.4 T, and the central radio frequency was set at $\omega_o/2\pi$ = 88.73 MHz for the ^{113}Cd nucleus and at $\omega_o/2\pi$=52.485 MHz for the ^{133}Cs nucleus. The spin-lattice relaxation time T_1 in the laboratory frame was measured by applying the pulse sequence $(\pi/2)_{sat}$–t–π/2. The width of the π/2 pulse for ^{113}Cd was 4.4 μs, and the signals were accumulated over 20–720 scans with a pulse delay of 10–120 s. The ^{113}Cd NMR spectra were obtained using various scan numbers owing to lower intensity according to the temperature. The width of the π/2 pulse for ^{133}Cs was 6.5 μs. The saturation recovery traces for Cs and Cd in $CsCdBr_3$ are shown for delay times ranging from 1 s to 1500 s. The temperature- dependent NMR measurements were performed between 180 and 410 K. Unfortunately, the relaxation times could not be determined above 420 K and below 180 K because the NMR spectrometer was unable to provide adequate temperature control at higher and lower temperatures. The sample temperature was maintained at constant values with an accuracy of ±0.5 K by controlling the nitrogen gas flow and heater current. The heating rate during the temperature changes was 1 K/min, and each temperature was maintained for approximately 5 min before the NMR measurements.

Results and Discussion

The structure of the $CsCdBr_3$ crystal at room temperature was determined with an X-ray diffraction system (Bruker AXS GMBH) at the Korea Basic Science Institute, Seoul Western Center. The structure of the $CsCdBr_3$ crystal exhibited hexagonal symmetry with the following cell parameters: a=b=7.6876 Å, c=6.7349 Å, α=β=90°, and γ=120°. These results are consistent with previously reported values.[18]

The ^{113}Cd nucleus, which has spin I=1/2, has a natural isotopic abundance of 12.3% and relatively high NMR sensitivity. Therefore, ^{113}Cd NMR spectroscopy has been used to examine the structures and dynamics of various inorganic and organic substances. The ^{113}Cd NMR spectrum for the $CsCdBr_3$ single crystal, obtained here through a solid-state NMR method, consists of one resonance line. The resonance frequency increased slowly and monotonously with increasing temperature, as shown in figure 2.

The saturation recovery traces for ^{113}Cd at all studied temperatures could be satisfactorily fitted with the single exponential function: $[M(\infty) - M(t)] / M(\infty) = A \exp(-Wt)$, where M(t) is the nuclear magnetization

at time t, and W is the transition probability corresponding to $\Delta m = \pm 1$. The spin-lattice relaxation rate is given by $1/T_1 = W$, and obtained for ^{113}Cd in the laboratory frame in the temperature range of 180~410 K. As shown in figure 3, the value of $1/T_1$ for ^{113}Cd in this single crystal increased with temperature, meaning that the geometry of the $CdBr_6^{4-}$ octahedra continued to change. The T_1 values at low temperatures are very large, at the order of 1000 s, while those at high temperatures are about 300 s smaller. The temperature dependency of the $1/T_1$ data can be described by Eq. (1):[19]

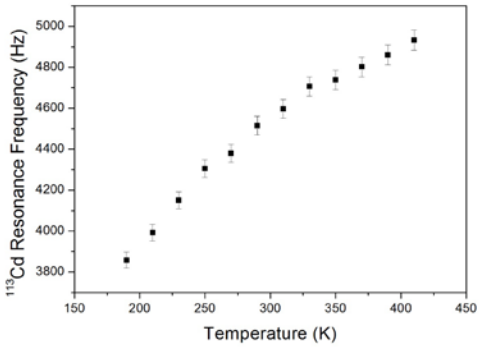

Figure 2. Resonance frequency of ^{113}Cd in $CsCdBr_3$ single crystals as a function of temperature.

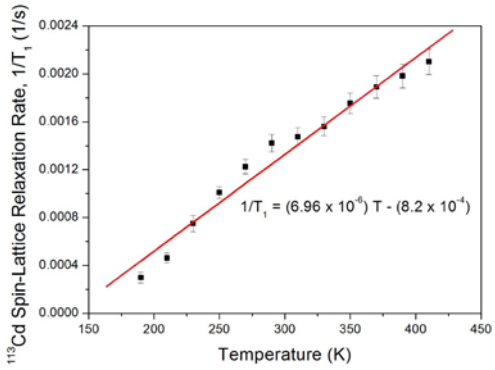

Figure 3. Spin-lattice relaxation rate $1/T_1$ for ^{113}Cd in $CsCdBr_3$ as a function of temperature. The solid line is a fit with the function $1/T_1 = aT+b$.

$$1/T_1 = aT^n + b \qquad (1)$$

where a and b are constants and T is the temperature. The obtained fitted curve, $1/T_1=(6.96 \times 10^{-6})T-(8.2 \times 10^{-4})$, is shown as the solid curve in figure 3.

^{133}Cs is a quadrupole nucleus with a nuclear spin of I =7/2. When this nucleus is located in a nonzero electric field gradient (EFG), it exhibits 2I resonance lines if the nuclear quadrupole interaction perturbs the Zeeman energy levels. When the crystal is rotated around its crystallographic axis, the crystallographically equivalent ^{133}Cs nuclei produce one central line and six satellite lines. This seven-line structure is the result of the aforementioned quadrupole interaction. The ^{133}Cs NMR spectrum for $CsCdBr_3$ single crystal is shown in figure 4(a) as a function of temperature. The zero point of the x-axis corresponds to the resonance frequency $\omega_o/2\pi=$ 52.485 MHz of the ^{133}Cs nucleus. All the satellite transitions are well resolved from the central line, and the central line has a higher signal intensity than the rest. The splitting between the resonance lines decreased slightly with increasing temperature, indicating a change in the EFG at the Cs sites, which in turn indicates that the atoms neighboring the ^{133}Cs nuclei were displaced as the temperature was changed. In addition, the central resonance frequencies in figure 4(a) are plotted in figure 4(b), showing that it increases with increasing temperature. The ^{133}Cs spin-lattice relaxation time T_1 in the laboratory frame was measured from static NMR, by applying $(\pi/2)_{sat}$–t–$\pi/2$ pulse sequences. The recovery traces of the magnetization were measured at different temperatures, and T_1 was measured at the central resonance line (shown in figure 4). When only the central line is excited, the magnetization recovery of the ^{133}Cs nuclei in $CsCdBr_3$ crystals does not follow a single exponential function, but can be represented by a combination of four exponential functions. The signal for $W_1 = W_2$, where W_1 and W_2 are the transition probabilities for $|\Delta m|=1$, 2, is given by [20]

$$[M(\infty) - M(t)]/M(\infty) = 0.048 \exp(-0.476W_1t) + 0.818 \exp(-1.333W_1t) + 0.050 \exp(-2.381W_1t) + 0.084 \exp(-3.810W_1t) \qquad (2)$$

where M(t) is the nuclear magnetization at time t. As shown in figure 5, the obtained $1/T_1$ increases with increasing temperature. At 290 K, T_1 is as long as 1448 s. According to our experimental results, the temperature dependence of $1/T_1$ for ^{133}Cs in $CsCdBr_3$ can be described approximately as $1/T_1=(5.17 \times 10^{-9})T^2 + (5.0 \times 10^{-5})$, which is shown as the solid curve in figure 5.

The interaction of the nuclear quadrupole moment

with the lattice vibrations represents a very important relaxation mechanism for nuclei with spin I $\geq$ 1 in many crystals. The coupling can generally be expressed by a spin - lattice Hamiltonian:[20]

$$\mathcal{H} = \sum_{q} F^{(q)} A^{(q)} \quad (3)$$

where $F^{(q)}$ and $A^{(q)}$ are the lattice and spin operators of order q, respectively. $F^{(q)}$ (hereafter we will omit the index q for brevity) can be expended in terms of the stress tensor σ:

$$F = F_o + F_1 \sigma + F_2 \sigma^2 + F_3 \sigma^3 + \ldots \quad (4)$$

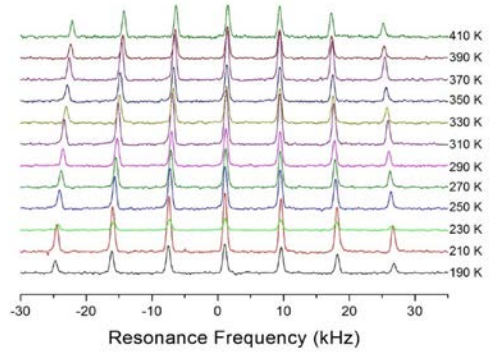

(a)

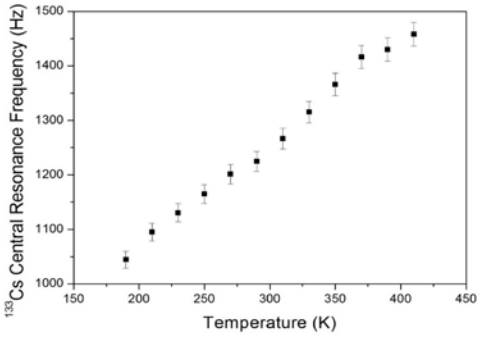

(b)

Figure 4. (a) ^{133}Cs spectrum in $CsCdBr_3$ single crystals as a function of temperature. (b) Central resonance frequency of ^{133}Cs in $CsCdBr_3$ single crystals as a function of temperature.

At temperatures far below the melting temperature of the crystal, we can expect the thermal stress to be small, so only the first few terms in Eq. (4) are important. The first linear term F1σ represents the absorption or emission of a single phonon (direct process). The next term, $F_2\sigma^2$, indicates either the emission or absorption of two phonons, or the absorption of one phonon followed by the emission of another one (Raman process). In the direct process, the spin-lattice relaxation rate $1/T_1$ is proportional to the square of the frequency ω_o and the absolute temperature. The direct process might be effective at low temperatures, but is practically non-essential for the spin-lattice relaxation of nuclear spins with nuclear quadrupole moments. On the other hand, in the high-temperature limit, the Raman process dominates, since the corresponding relaxation rate is proportional to the square of temperature. It should be noted that the direct and Raman processes (with the perturbing Hamiltonians $F_1\sigma$ and $F_2\sigma^2$, respectively) are both first-order processes. It has also been suggested that a second-order contribution to the relaxation rate might come from the interference between the spin–lattice term $F_1\sigma$ and the anharmonic term $F_3\sigma^3$ in the lattice energy, being responsible for the thermal conductivity. The interference between higher order terms either in the spin–lattice coupling ($F_m\sigma^m$) or in the lattice energy ($G_m\sigma^m$) may also provide smaller contributions.

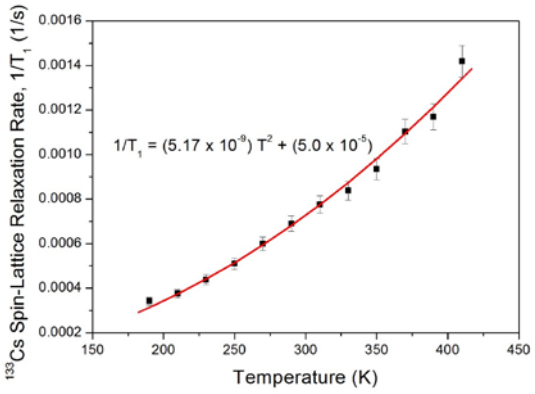

Figure 5. Spin-lattice relaxation rate $1/T_1$ for ^{133}Cs in $CsCdBr_3$ as a function of temperature. The solid line is a fit with the function $1/T_1 = aT^2+b$.

As discussed earlier, the spin-lattice relaxation rate for ^{113}Cd can be fitted by Eq. (1) with n=1, and therefore it can be explained in terms of single-phonon process for nuclear spin-lattice relaxation. Meanwhile, the experimentally obtained temperature dependence of $1/T_1$ for ^{133}Cs can be described by the simple power law $1/T_1 \propto T^2$. Such a relationship suggests that the Raman spin-phonon process is mainly responsible for the nuclear spin-lattice relaxation in ^{133}Cs.

Conclusions

The resonance frequencies and the spin-lattice relaxation rates ($1/T_1$) in ^{113}Cd and ^{133}Cs NMR spectra in the perovskite-type $CsCdBr_3$ single crystal were analyzed, and found to change continuously with temperature between 180 and 410 K. The changes in frequencies and $1/T_1$ observed in ^{113}Cd spectra were related to the changing structural geometry of the $CdBr_6^{4-}$ units, whereas those observed in ^{133}Cs spectra were related to change due to $CdBr_6^{4-}$. The relaxation rates for both ^{113}Cd and ^{133}Cs increased with increasing temperature, and can be described as $1/T_1 \propto T$ for ^{113}Cd and $1/T_1 \propto T^2$ for ^{133}Cs. Therefore, the dominant relaxation mechanisms for the ^{113}Cd and ^{133}Cs nuclei, which have electric dipole and quadrupole moments, respectively, are obtained by coupling these moments to the thermal fluctuations in the local EFG, namely via direct single phonon process for ^{113}Cd and Raman spin-phonon process for ^{133}Cs.

Acknowledgment

This research was supported by the Basic Science Research program through the National Research Foundation of Korea (NRF), funded by the Ministry of Education, Science and Technology (2015R1A1 A3A 04001077) and (2016R1A6A1A03012069).

References

1. F. Ramaz, R. M. Macfarlane, J. C. Vial, J. P. Chaminade, and F. Madeore, *J. Lumin.* **55**, 173 (1993)
2. O. G. Noel, P. Goldner, and Y. L. Du, *Spectrosc. Lett.* **40**, 247 (2007)
3. H.-Q. Wang, X.-Y. Kuang, and H.-F. Li, *Chem. Phys. Lett.* **460**, 365 (2008)
4. L. Kang, D. M. Ramo, Z. Lin, P. D. Bristowe, J. Qin, and C. Chen, *J. Mater. Chem.* **C1**, 7363 (2013)
5. M. G. Brik, and A. A. Chaykin, *J. Lumin.* **145**, 563 (2014)
6. B. Z. Malkin, A. I. Iskhakova, S. Kamba, J. Heber, M. Altwein, and G. Schaack, *Phys. Rev. B* **63**, 75104 (2001)
7. O. Guillot-Noel, Ph. Goldner, and D. Gourier, *Phys. Rev. A* **66**, 63813 (2002)
8. O. Guillot-Noel, Ph. Goldner, P. Higel, and D. Gourier, *J. Phys. Condens. Matter* **16**, R1 (2004)
9. M. Mujaji, and J. D. Comins, *Phys. Status Solidi C* **1**, 2372 (2004)
10. M. Karbowiak, A. Mech, and J. Drozdzynski, *Chem. Phys.* **308**, 135 (2005)
11. S. P. Huang, W.-D. Cheng, D.-S. Wu, X. D. Li, Y.-Z. Lan, F.-F. Li, J. Shen, H. Zhang, and Y.-J. Gong, *J. Appl. Phys*. **99**, 13516 (2006)
12. A. Ferrier, M. Velazquez, J.-L. Doualan, and R. Monwrge, *J. Appl. Phys.* **104**, 123513 (2008)
13. A. Ferrier, M. Velazquez, J.-L. Doualan, and R. Monocorge, *J. Lumin.* **129**, 1905 (2009)
14. Z.-X. Yan, X.-Y. Kuang, M.-L. Duan, C.-G. Li, and R.-P. Chai, *Mol. Phys.* **108**, 1899 (2010)
15. R. Demirbilek, R. Feile, and A.C. Bozdogan, *J. Lumin.* **161**, 174 (2015)
16. J. Neukum, N. Bodenschatz, and J. Heber, *Phys. Rev*. **B 50**, 3536 (1994)
17. Ph. Goldner, F. Pelle, D. Meichenin, and F. Auzel, *J. Lumin.* **71**, 137 (1997)
18. G. L. McPherson, A. M. McPherson, and J. L. Atwood, *J. Phys. Chem. Solids* **41**, 495 (1980)
19. A. Abragam, The Principles of Nuclear magnetism, Oxford University Press, Oxford (1961)
20. M. Igarashi, H. Kitagawa, S. Takagawa, R. Yoshizaki, Y. Abe, *Z. Naturforsch.* **A47**, 313 (1992)